Small-Angle X-Ray Scattering Studies on the X-Ray Induced Aggregation of Malate Synthase Computer Simulations and Models

Peter Zipper

Institut für Physikalische Chemie der Universität Graz, Heinrichstraße 28, A-8010 Graz, Austria

and

Helmut Durchschlag

Institut für Biophysik und Physikalische Biochemie der Universität Regensburg

Z. Naturforsch. **35 c**, 890–901 (1980); received November 12, 1979/July 14, 1980

Malate Synthase, Small-Angle X-Ray Scattering, X-Ray Induced Aggregation, Computer Simulations, Models for the Aggregation Process

Malate synthase undergoes an X-ray induced aggregation which can be monitored in situ by small-angle X-ray scattering; the analysis of scattering curves, taken at subsequent stages of aggregation, has led to the establishment of a tentative model for an aggregation in two dimensions (Zipper and Durchschlag (1980) Rad. and Environm. Biophys., in press).

This model was checked by comparison of appropriate theoretical curves with the experimental curves. The theoretical scattering curves for this comparison were obtained by weighted averaging over the scattering curves calculated for various species of hypothetical aggregates. Based on the approximation of the unaggregated enzyme particle by an oblate cylinder, the aggregates were assumed to be composed of 2, 3, 4 or 6 of such cylinders, associated side-by-side in one and later on in two linear rows. The weight fractions of the species were chosen so, that an optimum fit of the experimental mean radii of gyration and mean degrees of aggregation was achieved. The distance distribution functions calculated for the model are very similar to the functions derived from the scattering experiment. Cross-section Guinier plots of the scattering curves of the model reveal the occurrence of one and later on of two pseudo cross-section factors similar to those observed in the experimental scattering curves. The pseudo thickness factor of the model of the unaggregated particle is found to be retained in the model curves for all stages of aggregation. From these results it can be concluded that the model for the aggregation process is essentially consistent with the scattering behaviour of the aggregating enzyme. Small differences between the theoretical and experimental curves may be explained by the idealizations of the model. The comparison of theoretical curves for alternative models, assuming aggregation in three dimensions, suggests that these models are unlikely, though small amounts of three-dimensional aggregates cannot be ruled out completely.

Introduction

In preceding papers [1–3] we have demonstrated that upon prolonged X-irradiation of aqueous solutions of the enzyme malate synthase (EC 4.1.3.2) the enzyme undergoes an X-ray induced aggregation. Malate synthase was the first enzyme where the structure of the damaged enzyme particles was investigated by the small-angle X-ray scattering (SAXS) technique. It has been shown that the process of aggregation can be monitored in situ by a SAXS experiment, whereby the production of aggregates under the impact of the primary radiation and their investigation by means of the measurement of the scattered radiation are performed simultaneously.

The analysis of scattering curves taken at subsequent stages of aggregation of the enzyme has led to the following experimental findings:

1) The radius of gyration, the intensity scattered at zero angle and the extension of the distance distribution function were found to increase with the time of irradiation of the enzyme sample, thus reflecting the process of aggregation (*cf.* Fig. 1 a).

2) The pseudo thickness factor which occurs in the scattering curve of the native enzyme due to its oblate shape was found to be retained also during the aggregation, however, with a slight decrease of the radius of gyration of the thickness with proceeding aggregation.

Reprint requests to Dr. Peter Zipper.

0341-0382/80/1100-0890 $ 01.00/0

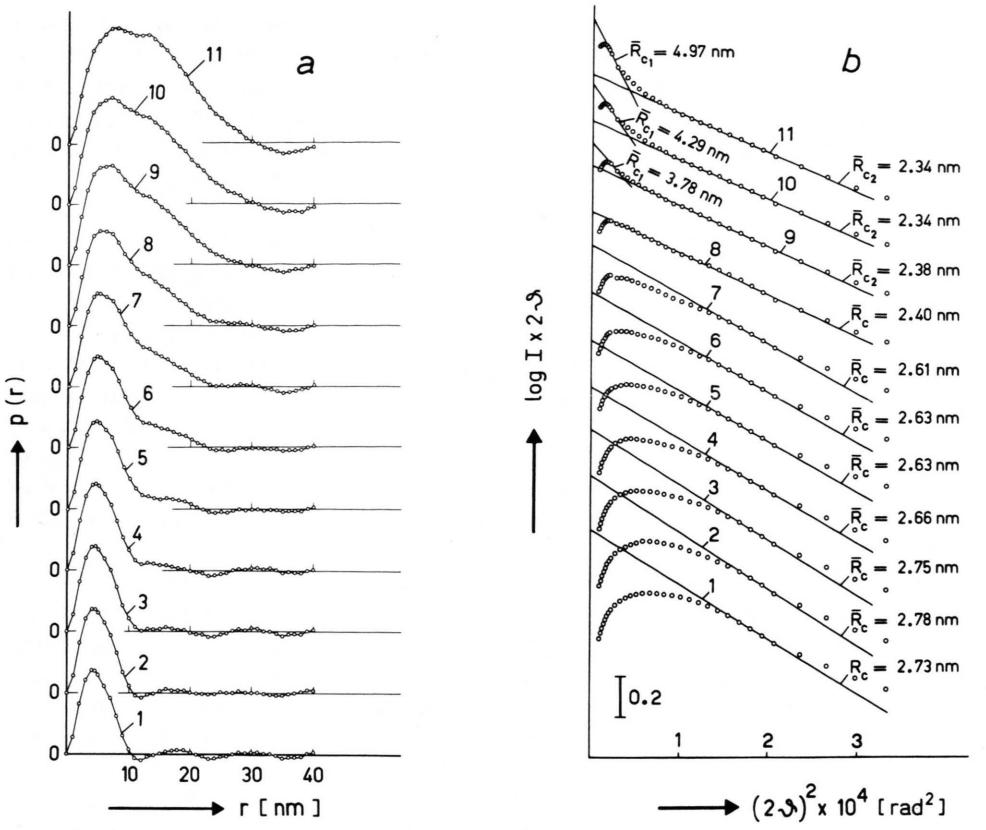

Fig. 1. Distance distribution functions $p(r)$ (a) and cross-section Guinier plots (b) of aggregating malate synthase as obtained from previous SAXS measurements [3]. Curves 1 refer to the unaggregated enzyme; subsequent curves were registered in time intervals of 5.7 h. $\bar{R}_c$: mean radius of gyration of the cross-section.

3) In cross-section Guinier plots of the scattering curves (*cf.* Fig. 1b), an extended linear range occurred after some time of irradiation of the enzyme sample. The slope of this range was found to correspond to a cross-sectional radius of gyration comparable to about the theoretical value for the native enzyme or for a linear row of side-by-side associated enzyme particles; it decreases slightly with proceeding aggregation. At later stages of aggregation a second and increasingly steeper linear range occurs in the cross-section Guinier plots at smaller scattering angles.

We have interpreted these findings in terms of a tentative model of the aggregation process. According to this model, the first step of aggregation would be a side-by-side association of enzyme particles in one dimension and this would be followed by a two-dimensional aggregation of the same kind. An aggregation in the third dimension, *i. e.* along the short axis of the oblate enzyme particles, was not assumed in the model.

In this paper, we present computer simulations to prove that the model is actually consistent with the experimentally observed scattering behaviour of the aggregating enzyme. We will also discuss some alternative models and show that these are much less compatible with the experimental data.

Together with the preceding experimental studies [1–3] this paper demonstrates the feasibility to elucidate the X-ray induced aggregation of proteins by means of the SAXS method. This opens a novel application of this technique in the field of radiation biology for the study of radiation damages of biopolymers. On the other hand, in conventional SAXS experiments which are performed to investigate biopolymers in the native state, the occurrence of radiation damages would be detrimental. Precautions and procedures by which the extent of

radiation damages can be reduced have also been shown up in refs. [2, 3] and are discussed in more detail in ref. [4]. Some of the precautions have already been applied successfully in the SAXS investigation of native substrate-free malate synthase and of various enzyme-substrate complexes [5].

Methods

A short survey of the theory of SAXS has been described in refs. [2, 3].

Results and Discussion

1. The model of two-dimensional aggregation

General remarks

The basic idea which underlies our model of the aggregation process is that the aggregation proceeds stepwise and the aggregates formed are stable for some time. As this concept does not rule out that aggregates from different steps of aggregation are present simultaneously, the SAXS results represent a superposition of various subsequent steps of aggregation. Therefore the analysis of the experimental SAXS curves cannot lead to an unambiguous picture of the aggregation, particularly at the later stages, but it may nevertheless reveal some general principles of the aggregation process.

To check whether our interpretation of the scattering behaviour of aggregating malate synthase is consistent with the experimental results, we have compared the experimental curves with theoretical curves. The theoretical curves for this comparison were obtained by averaging over the scattering curves calculated for models of various species of aggregates whereby appropriate weight fractions of the species were assumed.

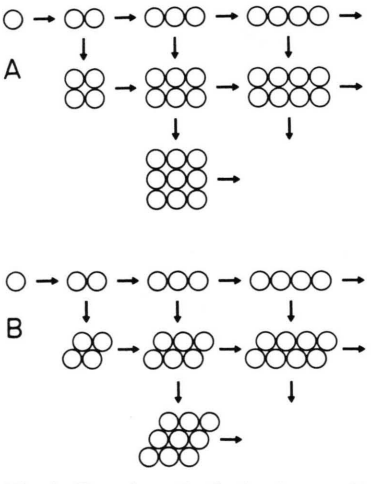

Fig. 2. Two hypothetical schemes (A, B) for side-by-side association of oblate rotational particles as established by the SAXS results on malate synthase.

In these calculations, for the unaggregated enzyme the cylindrical rather than the ellipsoidal model [1, 5] was chosen, mainly because of the closer agreement of its diameter with the experimentally determined diameter of the enzyme particle. Thus the unaggregated enzyme was represented by a circular cylinder of radius $r = 5.4$ nm and height $H = 3.6$ nm. Similarly, models for the various species of aggregates were composed of several of such cylinders. Only plane aggregates were taken into account.

Fig. 2 shows two hypothetical schemes for an aggregation in two dimensions. It is well known that onyl certain amino acids, namely those containing sulfur or aromatic rings, are particularly sensitive towards attacks by the products of water radiolysis. Those amino acids have already been found involved in protein cross-linking after irradiation (*cf.* ref. [6]). Accordingly, in an oligomeric enzyme, composed of identical subunits which contain those amino acids on the surface, each subunit will bear one or more potential "binding sites" which upon the impact of radiation may become able to form links between two subunits of the same enzyme particle or between two enzyme particles or their aggregates (*cf.* ref. [7]). Taking into account this regular distribution of potential binding sites on the enzyme surface, one may expect that the mutual arrangement of enzyme particles in an aggregate depends to some extent on the number of subunits per enzyme molecule.

Malate synthase was assumed to be composed of four subunits [8]. For this case aggregation scheme A holds (*cf.* Fig. 2). Recently some hints have been pointed out that malate synthase might consist of three rather than four subunits [9]. Therefore we have included in Fig. 2 a possible aggregation scheme allowing for that case (scheme B); this scheme is based on the assumption of two binding sites per subunit.

Model calculations were performed on the basis of both aggregation schemes and yielded similar results. In the calculations, besides the unaggregated

enzyme particle only the four lowest aggregates (dimer, trimer, tetramer, hexamer) * shown in Fig. 2 were taken into account. The scattering curves of the models for the aggregates were calculated by means of a computer program developed at the Graz institute [10]. Another computer program was developed to perform the weighted averaging over the scattering curves for the various species of aggregates. The calculations were performed on UNIVAC 494 and 1100/81 computers.

Simulation of the experimental radii of gyration and degrees of aggregation

The weight fractions of the various species were derived from the experimentally determined mean radii of gyration and mean degrees of aggregation as described in the following. The mean degree of aggregation $\bar{x}$ and the mean square of the radius of gyration $\overline{R^2}$ are related to the corresponding parameters x_i and R_i^2 and to the weight fractions w_i of the various species of particles according to (*cf.* ref. [3]):

$$\bar{x} = \sum w_i x_i \tag{1}$$

$$\overline{R^2} = \frac{\sum w_i x_i R_i^2}{\bar{x}}. \tag{2}$$

To approximate an experimental scattering curve by a model curve based on a limited set of species of particles, the weight fractions should be chosen so that both $\bar{x}$ and $\overline{R^2}$ of the model fit the corresponding experimental parameters. Since in our case the absolute values of the experimental mean radii of gyration might be systematically low due to the neglection of interparticular interference effects [3], it appeared to be more convenient to fit the ratio $\overline{R^2}/R_1^2$, where R_1 is the radius of gyration of the unaggregated enzyme particle. Values of $(R_i/R_1)^2$ for the various species of aggregates, as assumed in our aggregation model, are listed in Table I. Note that the values for the tetrameric and hexameric aggregates hold for both aggregation schemes, though the aggregates are of different shape.

Table I. Parameters x and $(R/R_1)^2$ for models of aggregates composed of circular cylinders of radius $r = 5.4$ nm and height $H = 3.6$ nm.

x	$(R/R_1)^2$	Way of association
1	1.0	
2	2.863	side-by-side, one-dimensional
3	5.969	
4	4.727	side-by-side, two-dimensional
6	7.832	
2	1.207	along the rotational axis

* In biochemical papers the terms monomer, dimer, trimer, tetramer, etc. are used to designate the number of subunits in an enzyme; in this paper these terms are applied to characterize in aggregates the number of enzyme particles, regardless of the number of their subunits.

Because of the neglection of interparticular interferences in the experimental scattering curves, we have chosen the experimental values of $\bar{x}_p$ and $\bar{R}_p$ * as derived from the distance distribution functions $p(r)$ (*cf.* Fig. 1a and ref. [3]) as basis for the computer simulation. The best fit of the data for the early stages of aggregation (runs 2–4, *cf.* Table II) was obtained when only dimers were assumed besides unaggregated particles and the weight fractions were chosen so as to fit perfectly the experimental $\bar{x}_p$. But even then the calculated ratios $\overline{R^2}/R_1^2$ were found to be slightly higher than the experimentally obtained ratios $(\bar{R}_p/R_1)^2$. However, as the discrepancies do not exceed a few percent, a monomer-dimer model can be assumed to be a sufficient approximation for the early stages of aggregation.

The data for the following runs, on the other hand, could not be approximated by a monomer-dimer model any longer, because in that case the theoretical ratios $\overline{R^2}/R_1^2$ would have been considerably smaller than the experimentally found ratios. Therefore further species of aggregates were included in the models, namely trimers and tetramers, and for runs 7–11 also hexamers. Since there exists no unique solution, it was necessary to assume reasonable weight fractions for one or two of the species. A set of models, based on the arbitrary assumption of a steady decrease of the weight fraction of the monomer, is shown in Fig. 3 and listed in Table II. It should be noted that the weight fractions assumed in these models hold for both aggregation schemes.

Fig. 4 presents Guinier plots of the innermost portions of the theoretical scattering curves of the models for runs 1–11 as calculated on the basis of aggregation scheme A. These curves have been computed down to zero angle, whereas in our SAXS

* The experimental mean radii of gyration $\bar{R}_G$ and $\bar{R}_p$ were defined in ref. [3] as square roots of z-averages, therefore, $\bar{R}_G^2$ and $\bar{R}_p^2$ represent like $\overline{R^2}$, as given by Eqn (2), z-averages.

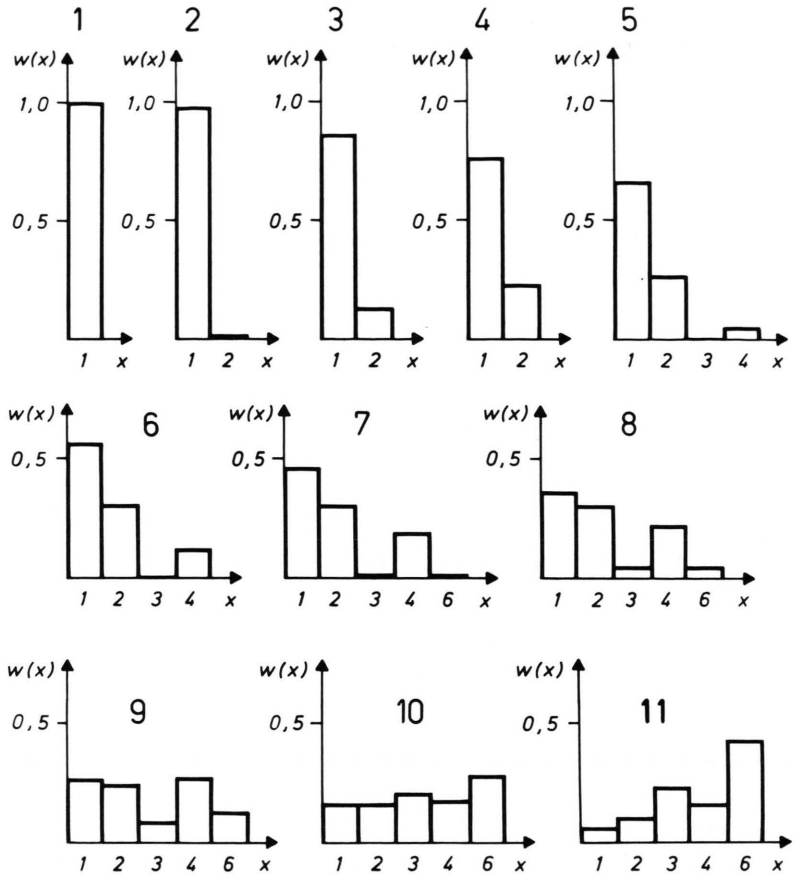

Fig. 3. The weight fractions $w(x)$ of x-mers as used in the calculation of model curves for the experimental runs 1–11. The weight fractions are derived from the experimental mean radii of gyration and the experimental mean degrees of aggregation of malate synthase as described in the text.

Table II. Comparison of the experimental parameters $\bar{x}_p$ and $(\bar{R}_p/R_1)^2$ with the parameters $\bar{x}_p$, $\bar{x}_G$, $(\bar{R}_p/R_1)^2$, $(\bar{R}_G/R_1)^2$ for models according to scheme A.

Run	Experiment [a]		Model				Weight fractions of models for aggregates				
	$\bar{x}_p$ [b]	$(\bar{R}_p/R_1)^2$ [b]	$\bar{x}_G$ [c]	$(\bar{R}_G/R_1)^2$ [c]	$\bar{x}_p$ [d]	$(\bar{R}_p/R_1)^2$ [d]	w_1	w_2	w_3	w_4	w_6
1	1.0	1.0	1.0	1.0	1.0	1.0	1.0				
2	1.02	1.03	1.02	1.06	1.02	1.07_5	0.98	0.02			
3	1.13_5	1.44	1.13	1.35	1.13_5	1.44	0.865	0.135			
4	1.23_5	1.64_5	1.23	1.58	1.23_5	1.70	0.765	0.235			
5	1.45_5	2.36	1.44	2.09	1.45	2.29_5	0.665	0.2696	0.0088	0.0566	
6	1.69	2.82	1.66	2.52	1.68	2.76	0.565	0.3049	0.0073	0.1228	
7	2.02	3.53	1.97	3.07	1.99	3.36	0.465	0.3043	0.0193	0.1913	0.02
8	2.34	4.13	2.27	3.54	2.29_5	3.90	0.365	0.3095	0.0510	0.2245	0.05
9	2.89	5.02	2.78	4.26	2.82	4.73	0.265	0.2442	0.0875	0.2732	0.13
10	3.53	6.08	3.35	5.08	3.42	5.70	0.165	0.1649	0.2093	0.1809	0.28
11	4.22	6.68	4.01	5.70	4.09	6.31	0.065	0.1043	0.2364	0.1643	0.43

[a] *cf.* ref. [3].
[b] Determined from the experimental distance distribution function $p(r)$; the theoretical mean degree of aggregation $\bar{x}$ of the models equals the experimental $\bar{x}_p$; the theoretical parameter $\bar{R}^2/R_1^2$ of the models equals the experimental $(\bar{R}_p/R_1)^2$, except the models for runs 2–4, where the theoretical ratios are 1.07_5, 1.44_5 and 1.71.
[c] Determined from the scattering curve of the model.
[d] Determined from the $p(r)$ function of the model.

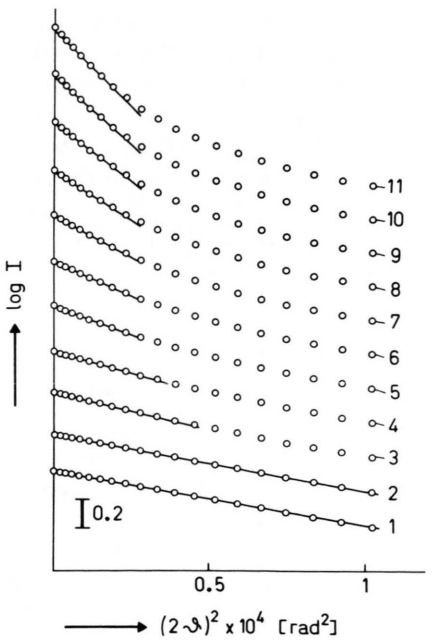

Fig. 4. Guinier plots of the scattering curves of models for the experimental runs 1–11. The models are based on scheme A and the weight fractions shown in Fig. 3. The approximation by straight lines was carried out in analogy to the treatment of the experimental curves and neglects all data from angles smaller than 3 mrad.

experiments the smallest angle at which measurements could be performed amounted to about 3 mrad [3]. Therefore, the approximation of the experimental curves according to Guinier's law did not include any data from angles smaller than 3 mrad. When the same procedure as for the approximation of the experimental curves was applied also to the theoretical curves in Fig. 4, the straight lines shown in the figure resulted. It can be seen that these straight lines are a very good approximation to the data for the models of the early stages of aggregation even at angles below 3 mrad. For the models of the most advanced stages of aggregation the quality of approximation in that angular range is not so good; therefore the values for $\bar{R}_G$ and $\bar{x}_G$ as derived from the slopes of the straight lines and from their intercepts on the ordinate are systematically low by a few percent.

For the Fourier transformation of the experimental scattering curves, the curves were extrapolated to zero angle from angles larger than about 3 mrad. Similarly, for the Fourier transformation of the theoretical curves of the models the extrapolated data for the innermost portion of the scattering curve were used instead of the correct intensities. The distance distribution functions $p(r)$ of the models as obtained in this way are shown in Fig. 5. The values for $\bar{x}_p$ and $\bar{R}_p$ of the models that can be derived from the $p(r)$ functions are much closer to the theoretical parameters than the values for $\bar{x}_G$ and $\bar{R}_G$ derived from the straight lines in Fig. 4 (*cf.* Table II). This better agreement justifies our choice of the experimental parameters $\bar{x}_p$ and $\bar{R}_p$ as the basis for the computer simulations of the aggregation model.

The distance distribution functions

The $p(r)$ functions in Fig. 5 for the models according to scheme A (solid curves) are very similar to the experimental $p(r)$ functions for aggregating malate synthase as shown in Fig. 1 a. Like those

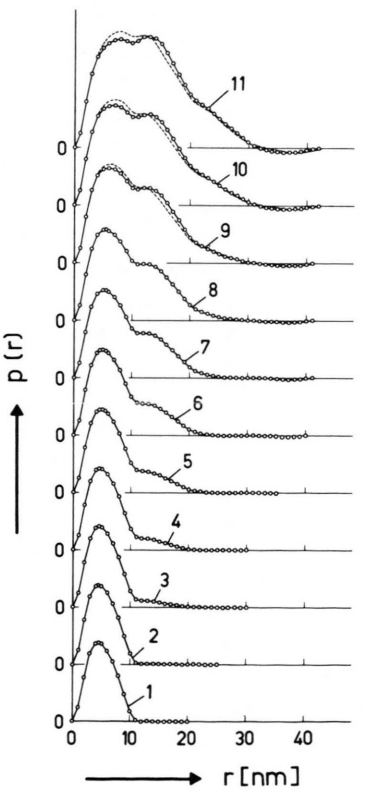

Fig. 5. Distance distribution functions $p(r)$ of models (solid curves: scheme A; dashed curves: scheme B) for the experimental runs 1–11. For the calculation of these curves, the scattering curves of the models were extrapolated to zero angle from $2 \geq 3$ mrad (*cf.* Fig. 4). The corresponding set of experimental $p(r)$ functions is shown in Fig. 1 a.

curves they show a gradual shift of the first zero from about 10 nm at the beginning to about 30 nm at last. It should be noted that this increase of the extension of the $p(r)$ function agrees well with the actual increase of the maximum particle diameter as given by the models (*cf.* Figs. 2 and 3). In contrast to the experimental curves which show a considerable oscillation around the base line after the first zero, such an oscillation is missing in the $p(r)$ functions of the models for the early stages of aggregation (curves 1–6 of Fig. 5). On the other hand, in the curves simulating the more advanced stages of aggregation a distinct minimum occurs after the first zero like in the experimental curves. Such a pronounced minimum does not occur when the correct intensities instead of extrapolated intensities are used for the Fourier transformation in the innermost portion of the scattering curve.

Thus the relatively deep minimum in the tail ends of the experimental $p(r)$ functions for runs 7–11 (*cf.* Fig. 1 a) is probably due to the limitation of the scattering curves by the resolution of the collimation system; the oscillations in the experimental $p(r)$ functions for runs 1–7 might be due to the neglection of interparticular interferences in the experimental scattering curves.

The model curves for the various stages of aggregation according to scheme A (Fig. 5, solid curves) show an inflection at about 11 nm which sharpens into a distinct minimum at about the same position at higher degrees of aggregation. A slight inflection occurs also at about 20 nm. This behaviour can be explained by the side-by-side association of cylinders as assumed in our aggregation model. According to the model (*cf.* Fig. 2), the cylindrical particles in an aggregate contact each other only along lines. For that reason there is much void between the associated particles which leads to a decrease of the frequency of certain distances within the aggregate as compared to a more homogeneous aggregate. A closer contact between the particles would reduce the amount of void and would lead therefore to more even $p(r)$ functions. The influence of void is demonstrated in Fig. 5 with some $p(r)$ functions (dashed curves) which were calculated on the basis of aggregation scheme B. In scheme B the tetramers and hexamers are more compact than in scheme A.

Also in the experimental $p(r)$ functions (Fig. 1 a), an inflection was found at about 11 nm in the curves for the highly aggregated enzyme. A second inflection was slightly indicated at large distances. These findings are consistent with the model of side-by-side aggregation of enzyme particles; however, the relative weakness of the experimentally observed effects seems to suggest that the aggregates are rather compact with less void between the associated enzyme particles than assumed in the obviously too idealized model.

The cross-section Guinier plots

Cross-section Guinier plots of the theoretical scattering curves of the models as calculated on the basis of scheme A are shown in Fig. 6. Also these plots look very similar to the corresponding plots of the experimental curves (Fig. 1 b). The approximation of the data by straight lines has been performed in analogy to the treatment of the experimental curves. Thus in the curves simulating the unaggregated enzyme and the early stages of aggregation (curves 1–7), a single straight line has been drawn through the data of the steepest region, *i. e.* between about 13 and 15 mrad. The cross-sectional radius of gyration $R_c = 2.61$ nm, that can be derived from the slope of the line through curve 1, is slightly smaller than the theoretical value of $R_c = 2.89$ nm for the cylindrical model, as calculated from the particle axes. It is also smaller than the corresponding experimental parameter which has been found to be $R_c = 2.73$ nm (*cf.* Fig. 1 b). Also the values for $\bar{R}_c$, as determined from curves 2–7, are somewhat lower than the experimentally obtained values. However, as in the plots of the experimental curves, the slopes of the lines through the data decrease slightly with increasing degree of aggregation.

Curve 8 of Fig. 6 can be approximated by a straight line over a wide angular range. This behaviour and the fact that the slope of this line is considerably smaller than the slopes of the lines in curves 1–7 are in best agreement with the experimental findings (*cf.* Fig. 1 b). However, the oscillation of the data points around the straight line is more pronounced in the theoretical curve than in the corresponding experimental curve. This oscillation, which occurs also in the theoretical curves 9–11, can be related like the inflections and the minimum in the $p(r)$ functions to the voids between the associated particles. Thus the only weak oscillation found in the experimental curves suggests once

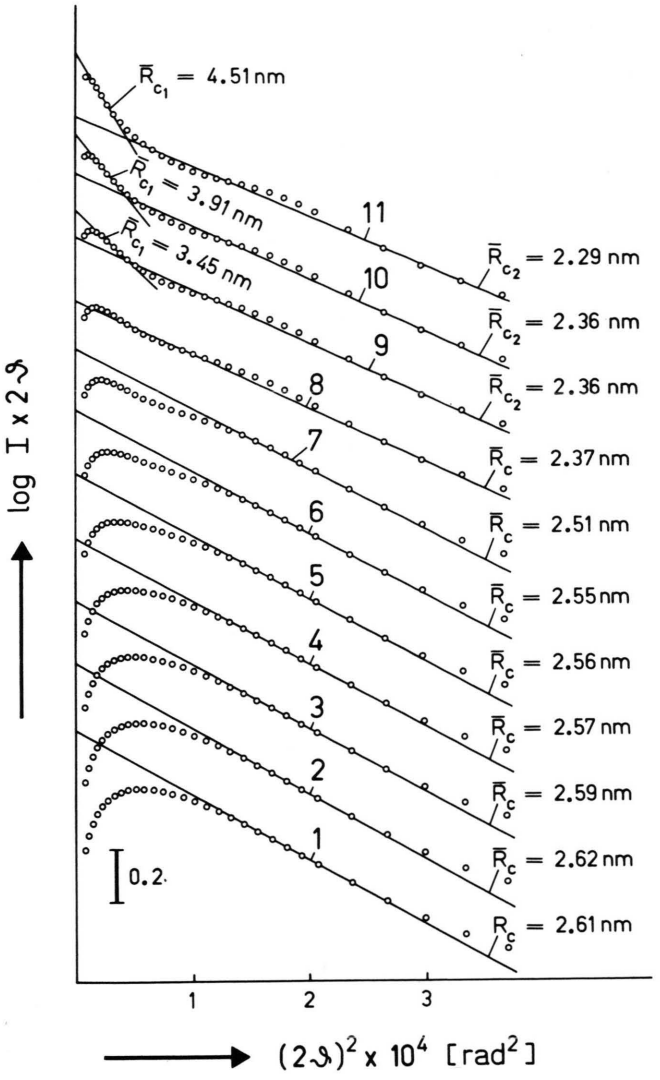

Fig. 6. Cross-section Guinier plots of the scattering curves of the models (scheme A) for the experimental runs 1–11. The corresponding set of experimental cross-section Guinier plots is shown in Fig. 1 b.

more that the aggregates of malate synthase are more compact than assumed in the model.

In curves 9–11 of Fig. 6, the intensity rises towards zero angle above the straight lines drawn through the outer part of the curves. This finding is again in best agreement with the experimental observations. It should be noted that such a significant increase of the intensity towards zero angle occurs only in the curves for those models which contain considerable amounts of hexamers, *i.e.* of two-dimensional elongate aggregates.

As in the experimental cross-section Guinier plots, the innermost portions of model curves 9–11 of Fig. 6 are also approximated by straight lines. However, the values for $\bar{R}_{c1}$ derived from their slopes are smaller than the corresponding experimental values. Possible reasons for this discrepancy might be the presence of larger amounts of such two-dimensional aggregates, as represented in the model by hexamers, and perhaps also the presence of even higher aggregates in the irradiated enzyme solution. However, an underestimation of the cross-section of the unaggregated enzyme particle by use of the cylindrical approximation would explain the difference between the cross-sectional radii of gyration as well. When the native enzyme particle is ap-

proximated by an ellipsoid of revolution, R_c of a two-dimensional aggregate of six such ellipsoids would be larger by about 9% than R_c of a hexamer composed of cylinders. On the other hand, the increase of voids in models composed of ellipsoids would give rise to even stronger oscillations of the scattering curves in cross-section Guinier plots and stronger inflections of the $p(r)$ functions than in the case of models based on the cylindrical approximation for the native enzyme particle.

The thickness Guinier plots

The thickness Guinier plots of the experimental scattering curves of aggregating malate synthase as shown in ref. [3] have demonstrated the obvious retention of the pseudo thickness factor as found for the native enzyme, however, with slightly decreasing mean radius of gyration of the thickness $\overline{R_t}$. The characteristic changes of the experimental curves during aggregation can be seen quite clearly in Fig. 7a, which shows a comparison of thickness Guinier plots of the curves from runs 1, 6 and 11. Thickness Guinier plots of the theoretical scattering curves for the corresponding models according to scheme A are shown in Fig. 7b. It is obvious that Figs. 7a and 7b have some features in common, as for instance at the smallest angles the decrease of the positive initial slope with proceeding aggregation. According to the models, this behaviour is related to the presence of extended disk-like aggregates.

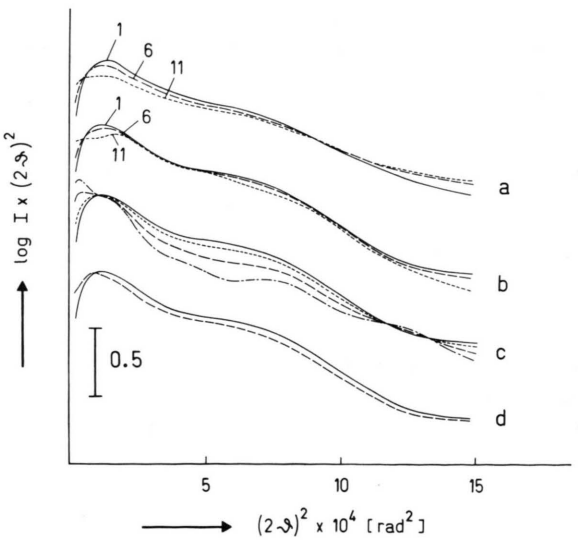

Fig. 7. Thickness Guinier plots of experimental and theoretical scattering curves. a) Experimental curves from runs 1, 6, and 11; b) theoretical curves for the corresponding models (scheme A); c) theoretical curves for a mixture of cylinders I and II; I: $r = 5.4$ nm, $H = 3.6$ nm, II: $r = 10.8$ nm, $H = 7.2$ nm; (——) $w_{II} = 0$, (- - - -) $w_{II} = 0.1$, (– –) $w_{II} = 0.3$, (–·–·) $w_{II} = 0.5$; d) theoretical curves for a mixture of cylinders I and III; I: $r = 5.4$ nm, $H = 3.6$ nm, III: $r = 16.2$ nm, $H = 10.8$ nm; (——) $w_{III} = 0$, (– –) $w_{III} = 0.13$.

The model curves almost coincide in the contiguous region between 15 and 22 mrad, but show another systematic variation at larger angles, namely a decrease of intensity with proceeding aggregation. On the contrary, in the experimental curves the intensity decreases with proceeding aggregation in the angular range from about 10 to 30 mrad, whereas it increases at larger angles. Obviously this gradual flattening of the experimental curves, which has been interpreted in ref. [3] in terms of a decrease of $\overline{R_t}$, cannot be simulated by the models assumed.

Reasons for this decrease of $\overline{R_t}$ might be an actual decrease of the particle thickness, as for instance caused by partial unfolding or degradation of the particles. Moreover, if degradation or dissociation to subunits due to X-irradiation occurs, the presence of considerable amounts of fragments or subunits of enzyme particles in the irradiated solution would also lead to a flattening of the scattering curves in the thickness Guinier plots. Preliminary investigations of irradiated enzyme by means of SDS polyacrylamide gel electrophoresis have shown that a cleavage of peptide chains upon X-irradiation actually occurs [11].

Simulation of aggregation by computer

It should be mentioned that results very similar to those shown in Figs. 4–7 were obtained when the aggregation process itself was simulated according to our model by means of a computer and the weight fractions of the various species of aggregates, including also much higher aggregates, were taken from this simulation. Only the differences between the theoretical values for $\bar{x}$ and $\overline{R^2}$ and the parameters derived from the scattering curves and the $p(r)$ functions of the models were found to be somewhat larger than with the model curves presented in this paper, probably due to the inclusion of larger aggregates in the model. Also these computer simulations demonstrated that the proposed model is essentially consistent with the experimentally observed scattering behaviour of aggregating malate synthase.

2. Alternative models

Aggregation in three dimensions

It remains to ask whether the proposed model for the aggregation process is unique or whether alternative interpretations of the experimental curves are also possible. One question appears to be of particular interest, namely whether an aggregation in the third dimension, *i. e.* along the rotational axis of the enzyme particle, can actually be ruled out. To answer this question, we have performed some additional model calculations.

We recall that the theoretical $\overline{R^2}/R_1^2$ ratios of the monomer-dimer models for the early stages of aggregation are slightly larger than the experimentally obtained ratios. If we assume that this discrepancy is due to the occurrence of an aggregation also along the rotational axis of the enzyme particle, we can easily calculate the weight fraction of such dimers, which is necessary in order to reduce the theoretical $\overline{R^2}/R_1^2$ to the experimental value. When this estimation is performed by using the experimental data from run 4 (*cf.* Table II), a weight fraction of 0.024 results. With 0.235 being the weight fraction of all dimers, the above result would mean that in only about 10% of the dimers the aggregation could have occurred along the rotational axis.

To study the possible influence of three-dimensional aggregation on the thickness Guinier plots, we have calculated the theoretical scattering curves for various models composed of only two species of particles, namely of the same cylinder as used for the model of the native enzyme particle ("cylinder I") and of a cylinder of the same axial ratio but being two or three times as large. A double-sized cylinder ("cylinder II") would represent a three-dimensional octamer. Thickness Guinier plots of the scattering curves for various weight fractions of such three-dimensional aggregates are shown in Fig. 7 c. As can be seen, the curves change systematically with increasing weight fraction of the large cylinder, namely the intensity increases at angles below about 10 mrad, and decreases at larger angles, apart from a narrow region in the tail end, where the curves almost coincide. Thus the presence of increasing amounts of particles of twice the thickness of the native enzyme is clearly reflected by an increase of the slope of the curves in the range at about 15 mrad. In the experimental curves, on the other hand, a decrease of the slope in this range with proceeding aggregation can be observed (*cf.* Fig. 7 a). Thus the thickness Guinier plots of the experimental curves give no hint for the presence of particles of twice the thickness of the native enzyme. Nevertheless, taking into consideration a possible compensation of the effects due to three-dimensional aggregation by the opposite effects due to degradation as discussed above, the presence of small amounts of aggregates with a thickness twice as large as that of the native enzyme cannot be ruled out definitely by our SAXS measurements.

The detection of small amounts of aggregates of still larger thickness by means of thickness Guinier plots would be practically impossible, because the thickness of such particles would lead to an increase of intensity only in the innermost portion of the scattering curves. Fig. 7 d shows a comparison of the scattering curve of the cylindrical model for the unaggregated enzyme particle with the scattering curve for a model consisting of a mixture of the aforementioned small cylinder I and a cylinder being three times as large ("cylinder III"). The weight fraction of the large particle was chosen so that $\bar{x}$ as derived from the $p(r)$ function is about the same as the corresponding experimental parameter for run 11. As can be seen from Fig. 7 d, the presence of the large particle only leads to a slight increase of intensity at the smallest angles, while over the rest of the angular range the intensity is systematically lower than in the curve for the unaggregated particle. $\overline{R_t}$ does not change by this decrease of intensity, because, apart from the region at the smallest angles, the two curves are practically parallel to each other.

The $p(r)$ function itself of this model (Fig. 8) differs significantly from those shown previously. In

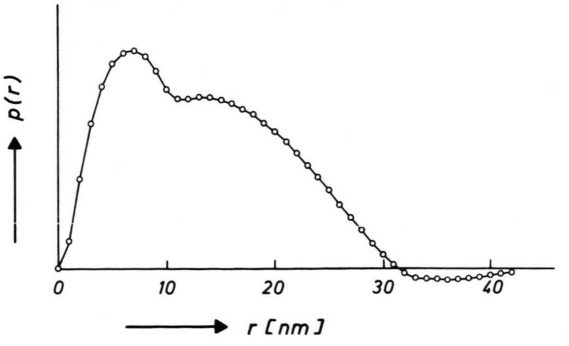

Fig. 8. Distance distribution function $p(r)$ for a mixture of cylinders I and III (*cf.* Fig. 7 d); $w_{III} = 0.13$.

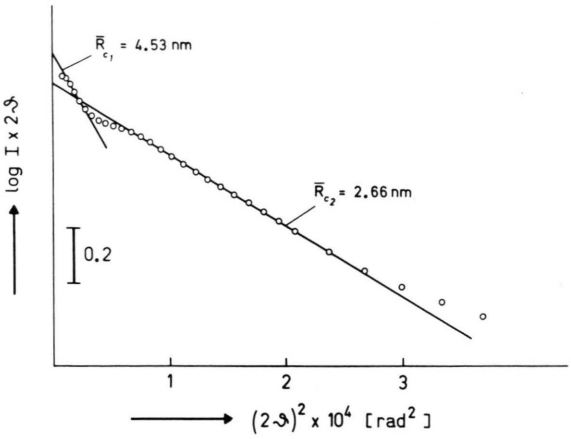

Fig. 9. Cross-section Guinier plot of the scattering curve for a mixture of cylinders I and III (*cf.* Fig. 7 d); $w_{III} = 0.13$.

contrary to the experimental $p(r)$ function for run 11 (Fig. 1 a) or to the $p(r)$ functions of the previous models for schemes A and B (Fig. 5), there is a reduced frequency of distances between 7 and 16 nm and an increased frequency of larger distances.

In a similar way the comparison of the cross-section Guinier plot (Fig. 9) of the scattering curve for this two-species model with the corresponding plot of the experimental curve from run 11 (Fig. 1 b) reveals significant differences. The range between 8 and 15 mrad is much steeper than in the experimental curve and corresponds to a $\bar{R}_{c2}$ of 2.66 nm as compared to the experimental value of 2.34 nm. Accordingly, the increase of intensity above the straight line towards the smallest angles is much less pronounced than in the experimental curve.

These findings clearly rule out this two-species model as a satisfying approximation of the experimentally observed scattering behaviour of the most aggregated enzyme sample. On the other hand, models similar to this two-species model would have to be taken into consideration in case our basic assumption fails to hold that the SAXS method delivers a superposition of various subsequent steps of aggregation. If for instance the intermediately formed aggregates are very unstable and the aggregation, once started, proceeds rapidly to large aggregates, then small aggregates would be present only in very low concentrations and would not significantly influence the scattering behaviour. In this case the scattering phenomenon would be essentially caused by a mixture of unaggregated enzyme and of large aggregates.

Model calculations, performed for this case, demonstrated that such models can be ruled out inter alia for the following reasons. Already for low values of $\bar{x}$ the first zero in the $p(r)$ functions of such models occurs at a distance corresponding to about the diameter of the large aggregates. This holds even when the innermost portion of the scattering curve is extrapolated from larger angles in about the same way as in the experimental scattering curves. Accordingly, the ratio $(\bar{R}_p/R_1)^2$ is particularly at low and medium $\bar{x}$ values much larger than the ratio observed experimentally at the same $\bar{x}$. Even if we take into consideration that in the experimental $p(r)$ functions the oscillations might have obscured a shift of the first zero to larger distances, the discrepancies between the experimental $(\bar{R}_p/R_1)^2$ ratios and the ratios as obtained from the $p(r)$ functions of the models let appear these models to be highly unlikely.

Conclusions

The computer simulations presented in the foregoing have demonstrated that the proposed model for an aggregation in two dimensions (*cf.* ref. [3]) is consistent in its essential implications with the experimentally observed scattering behaviour of aggregating malate synthase. The fact that the model is not always able to simulate perfectly the experimental curves is not surprising in view of the simple and highly idealized assumptions on which the model is based. For practical reasons the simplest possible models for the unaggregated enzyme and for the various species of aggregates have been chosen, *i. e.* an oblate circular cylinder was used as a model for the unaggregated enzyme and a regular arrangement of such cylinders was assumed in the aggregates. The experimental findings do not necessarily exclude slightly other shapes for the unaggregated enzyme (*cf.* [5]) and for the aggregates. However, the essential conclusions drawn from the calculations would not depend much on identity and number of subunits of the enzyme, and on the binding sites for the cross-linking the number of which can only be speculated about. Alternative models of this kind would also lead to the principle statement, that the aggregation process starts with an association of enzyme particles in one dimension, an event which is continued as a two-dimensional aggregation. An aggregation in the third dimension

does not occur to a considerable extent during the first steps of the aggregation process monitored by our SAXS experiment. The dominance of two-dimensional aggregation, at least during the first stages of aggregation, suggests that the binding sites for cross-linking are situated on the periphery of the oblate enzyme particles. This conclusion is discussed in refs. [2, 4] in connection with inactivation experiments.

The calculation of model curves has shown that the experimental SAXS curves of aggregating malate synthase reflect the scattering from mixtures of unaggregated enzyme and various species of small aggregates rather than from mixtures of unaggregated enzyme and very large aggregates. This finding is in accord with the results of the radiation-induced aggregation of other proteins (*cf.* [12–14]).

Acknowledgements

We wish to express gratitude to Professor Dr. J. Schurz, Graz, and to Professor Dr. R. Jaenicke, Regensburg, for their interest in the problem. H. D. thanks the Deutsche Forschungsgemeinschaft for support.

[1] P. Zipper and H. Durchschlag, Biochem. Biophys. Res. Commun. **75,** 394–400 (1977).
[2] P. Zipper and H. Durchschlag, Rad. Environm. Biophys., in press (1980).
[3] P. Zipper and H. Durchschlag, Monatsh. Chem., in press (1980a).
[4] P. Zipper and H. Durchschlag, Monatsh. Chem., in press (1980b).
[5] P. Zipper and H. Durchschlag, Eur. J. Biochem. **87,** 85–99 (1978).
[6] O. Yamamoto, Advances in Experimental Medicine and Biology, **Vol. 86 A,** (M. Friedman, ed.), pp. 509–547, Protein Crosslinking. Biochemical and Molecular Aspects, Plenum Press, New York, London 1977.
[7] V. Jakubick and H. Delincée, Z. Naturforsch. **33 c,** 203–209 (1978).
[8] G. Schmid, H. Durchschlag, G. Biedermann, H. Eggerer, and R. Jaenicke, Biochem. Biophys. Res. Commun. **58,** 419–426 (1974).
[9] H. Durchschlag, F. Bogner, D. Wilhelm, R. Jaenicke, P. Zipper, and F. Mayer, Hoppe-Seyler's Z. Physiol. Chem. **359,** 1077 (1978).
[10] O. Haager, unpublished results.
[11] H. Durchschlag and P. Zipper, Hoppe-Seyler's Z. Physiol. Chem. **361,** 239 (1980).
[12] H. Schüssler and H. Jung, Z. Naturforsch. **22 b,** 614–621 (1967).
[13] H. Delincée and V. Jakubick, Int. J. Appl. Radiat. Isotopes **28,** 939–945 (1977).
[14] M. R. Majewska and A. M. Dancewicz, Studia Biophysica **63,** 65–74 (1977).